

Electroweak Phase Transition in 2HDM under Higgs, Z-pole, and W precision measurements

Huayang Song^a, Wei Su^b, Mengchao Zhang^c

^a*CAS Key Laboratory of Theoretical Physics, Institute of Theoretical Physics, Chinese Academy of Sciences, Beijing 100190, P.R.China*

^b*Korea Institute for Advanced Study, Seoul 02455, Korea*

^c*Department of Physics and Siyuan Laboratory, Jinan University, Guangzhou 510632, P.R. China*

E-mail: huayangs@itp.ac.cn, weisu@kias.re.kr, mczhang@jnu.edu.cn

ABSTRACT: In this work we revisit the existence of a strong first order electroweak phase transition (SFOEWPT) and recent m_W precision measurement in the Type-I and Type-II 2HDMs. The $\mathcal{O}(100)$ GeV new scalars in 2HDMs are favored by SFOEWPT, which is necessary for electroweak baryogenesis, and observed m_W shift as well. We find that under current constraints, both Type-I and Type-II 2HDM can explain the SFOEWPT, Z-pole, Higgs precision measurements and m_W precision measurement of CDF-II at same time, and all these precision measurements are sensitive to heavy Higgs mass splitting in 2HDM. The allowed regions are $\Delta m_{A/C} \in (-400, 400)$ GeV, $\tan \beta \in (1, 50)$, and $\Delta m_{A/C} \in (-200, 300)$ GeV, $\tan \beta \in (1, 12)$ for Type-I and Type-II 2HDM respectively. Furthermore future lepton collider measurements on Higgs and Z boson properties can explore this scenario in more detail or even rule out it.

Contents

1	Introduction	1
2	2HDM	3
2.1	A Review	3
2.2	Theoretical Constraints on 2HDMs	3
2.3	Direct searches at LEP and LHC	4
2.4	Z-pole and Higgs precision measurements	5
2.5	m_W in the 2HDM	6
2.6	Flavour constraints	7
2.7	Phase transition in the 2HDM	7
3	Study results	8
3.1	Study method	8
3.2	SFOEWPT under LHC measurements	10
3.3	SFOEWPT under Higgs, Z and W precision measurements	10
4	Conclusion	11

1 Introduction

With the discovery of the Higgs boson at the Large Hadron Collider (LHC) in 2012 [1, 2], particle physics has been entering a new era. Due to the lack of direct search result at LHC, precision studies of particle physics are becoming important. The current measurements of particle properties seem to be consistent with all other categories of experiments and can be described by the Standard Model (SM) quite well. Meanwhile there are compelling arguments, both from theoretical and observational viewpoints, in favor of new physics beyond the Standard Model (BSM). The CDF collaboration has recently reported a precise measurement of the W boson mass, which indicates a significant tension with the previous measurements and the SM prediction [3]. Although this result needs to be further confirmed by other experiments, such as D0, ATLAS, and CMS, it is still an exciting possible signal indicating the existence of new physics at a place not far above the electroweak (EW) scale ¹.

Given this possible signal, the following question is which new physics does this possible signal point to. Among different kinds of BSM new physics, electroweak baryogenesis (EWBG) [12, 13] is likely to be relevant to the current possible signal. EWBG was proposed to explain the observed baryon asymmetry of the universe (BAU). Through the baryon

¹Recent study on the new CDF result see [4–11].

number breaking sphaleron process [14–16] and CP violated scattering with bubble wall, net baryon number can be produced during the nucleation process of Higgs field. To trigger the nucleation process and to prevent the generated net baryon being washed out, the electroweak phase transition (EWPT) needs to be a strong first order phase transition. However, due to current measured Higgs mass, the SM EWPT is not even first order [17, 18].

Therefore new particles are definitely required for a strong first order electroweak phase transition (SFOEWPT). Furthermore, new particles that help to trigger SFOEWPT can not be too heavy than EW scale, otherwise they will be decoupled in the thermal phase transition process and lose effect. Thus, the new measure W boson mass might be a hint of EWBG.

One method to trigger SFOEWPT is augmenting the SM Higgs sector via additional scalars, and it has been studied intensively in the literature [19–31]. Extending the Higgs sector by a singlet scalar seems to be the simplest choice, but it is difficult for such model to explain the observed m_W under current limits [32]. In this work we choose Two-Higgs-Doublet Models (2HDMs) [33, 34], which extend the SM Higgs sector by another doublet, as the benchmark model to study the relationship between SFOEWPT and m_W . After electroweak symmetry breaking, in addition to the SM-like Higgs boson h , there are three non-SM Higgs bosons, $H/A/H^\pm$, which can have masses below TeV and couple to the SM-like Higgs h to build an energy barrier between the symmetric and broken phase. Therefore the EW phase transition can be first order and strong enough for the baryogenesis [27]. Furthermore, these light extra scalar can induce a positive m_W shift [35] and modify the predictions on the Z -pole observables like the oblique parameters S , T and U via one-loop contributions to the W and Z self-energies. The mixing between neutral scalars and extra loop corrections further reduce the Higgs couplings $\kappa_i = g_{hii}^{2\text{HDM}}/g_{hii}^{\text{SM}}$ relative to their SM expectations. Though the LHC measurements still give a large amount of available phase space of the 2HDM, future Higgs factories, e.g. ILC [36], FCC-ee [37, 38] and CEPC [39, 40] can measure them with unprecedented precision to further constrain the model.

In this paper, we study the constraints from precision measurements (especially the new W boson mass and future Higgs coupling measurements) on the 2HDM and explore the possible parameter space which could lead to a SFOEWPT. Our study shows that SFOEWPT is consistent with the new uplifted m_W in a certain parameter space. But due to the close connection between m_W and other precise measurements, the “SFOEWPT + m_W ” scenario is in slight tension with current limits. Furthermore, the future precision lepton collider measurements of both Higgs and Z boson properties could fully rule out the alive parameters to fulfil SFOEWPT and m_W , provided the measured central values locate in the SM prediction. Conversely, if the “SFOEWPT + m_W ” scenario in 2HDM is true, than a clear deviation from SM prediction will be observed at future lepton colliders.

The rest of the paper is organized as follows. In Section 2 we briefly introduce 2HDM models and related constraints. Description on EWPT is also given in Section 2. In Section 3 we perform parameter space scan on a wide range and present alive points, with future precise measurements included. We conclude this work in Section 4.

2 2HDM

2.1 A Review

In this section, we provide a brief review of the aspects of 2HDMs. For pedagogical introduction, see Ref. [34] and a recent review Ref. [41] in light of current experiments. The scalar sector of 2HDMs consists two $SU(2)_L$ doublets Φ_i , $i = 1, 2$, which can be parameterized as below,

$$\Phi_i = \begin{pmatrix} \phi_i^+ \\ (v_i + \phi_i^0 + iG_i)/\sqrt{2} \end{pmatrix} \quad (2.1)$$

where v_1 and v_2 are the vacuum expectation values (VEVs) of the neutral components, satisfying the relation $v \equiv \sqrt{v_1^2 + v_2^2} = 246$ GeV. Assuming CP-conserving and only a soft breaking of a discrete \mathcal{Z}_2 symmetry allowed, the most general Higgs potential can be expressed as,

$$\begin{aligned} V^0(\Phi_1, \Phi_2) = & m_{11}^2 \Phi_1^\dagger \Phi_1 + m_{22}^2 \Phi_2^\dagger \Phi_2 - m_{12}^2 (\Phi_1^\dagger \Phi_2 + h.c.) + \frac{\lambda_1}{2} (\Phi_1^\dagger \Phi_1)^2 + \frac{\lambda_2}{2} (\Phi_2^\dagger \Phi_2)^2 \\ & + \lambda_3 (\Phi_1^\dagger \Phi_1) (\Phi_2^\dagger \Phi_2) + \lambda_4 (\Phi_1^\dagger \Phi_2) (\Phi_2^\dagger \Phi_1) + \frac{\lambda_5}{2} \left[(\Phi_1^\dagger \Phi_2)^2 + h.c. \right]. \end{aligned} \quad (2.2)$$

where there are eight real parameters, $\{m_{11}^2, m_{22}^2, m_{12}^2, \lambda_1, \lambda_2, \lambda_3, \lambda_4, \lambda_5\}$. After the electroweak symmetry breaking (EWSB), the scalar sector of a 2HDM consists of five mass eigenstates: a pair of neutral CP-even Higgses, h and H , a CP-odd Higgs, A , and a pair of charged Higgses H^\pm . We can express these states as,

$$\begin{aligned} h &= -s_\alpha \phi_1 + c_\alpha \phi_2, & A &= -s_\beta \varphi_1 + c_\beta \varphi_2, \\ H &= c_\alpha \phi_1 + s_\alpha \phi_2, & H^\pm &= -s_\beta \phi_1^\pm + c_\beta \phi_2^\pm. \end{aligned} \quad (2.3)$$

where we will identify h with the discovered SM-like 125 GeV Higgs without loss of generality.

For convenience, we will parametrize the potential of 2HDMs by the physical Higgs masses m_h, m_H, m_A and m_{H^\pm} , the mixing angle between the two CP-even Higgses α , $\tan \beta \equiv v_2/v_1$, the electroweak VEV v , and the soft \mathcal{Z}_2 symmetry breaking parameter m_{12}^2 . Note that the vacuum expectation value v and the mass of the SM-like Higgs, m_h are fixed to their known values 246 GeV and 125 GeV respectively, leaving the remaining six independent parameters.

Assigning different \mathcal{Z}_2 parities to the SM fermions, there are four types of 2HDMs. However, in this study, we focus on the so-called Type-I and Type-II 2HDMs, where all fermions obtain their masses from a single Higgs doublet in Type-I model while up- and down-type fermions obtain their masses from different Higgs doublets in Type-II model. In the Type-II model the couplings between A/H and down-type fermions are enhanced by $\tan \beta$ and therefore it is usually more constrained by experiments when $\tan \beta$ is large.

2.2 Theoretical Constraints on 2HDMs

The parameter spaces of 2HDMs are already constrained by theoretical consideration without experimental results.

- **Vacuum stability** In order to make the vacuum stable, the scalar potential should be bounded from below [42]:

$$\lambda_1 > 0, \lambda_2 > 0, \lambda_3 > -\sqrt{\lambda_1 \lambda_2}, \lambda_3 + \lambda_4 - |\lambda_5| > -\sqrt{\lambda_1 \lambda_2} \quad (2.4)$$

- **Perturbativity and unitarity** Requiring perturbativity, we must have $|\lambda_i| \leq 4\pi$. And requiring tree-level unitarity of the scattering in the 2HDM scalar sector imposes the following additional mass constraints [43]:

$$\left| 3(\lambda_1 + \lambda_2) \pm \sqrt{9(\lambda_1 - \lambda_2)^2 + 4(2\lambda_3 + \lambda_4)^2} \right| < 16\pi, \quad (2.5)$$

$$\left| (\lambda_1 + \lambda_2) \pm \sqrt{(\lambda_1 - \lambda_2)^2 + 4\lambda_4^2} \right| < 16\pi, \quad (2.6)$$

$$\left| (\lambda_1 + \lambda_2) \pm \sqrt{(\lambda_1 - \lambda_2)^2 + 4\lambda_5^2} \right| < 16\pi, \quad (2.7)$$

$$|\lambda_3 + 2\lambda_4 \pm 3\lambda_5| < 8\pi, \quad |\lambda_3 \pm \lambda_4| < 8\pi, \quad |\lambda_3 \pm \lambda_5| < 8\pi \quad (2.8)$$

To understand these constraints, it is useful to consider the relations between the quartic couplings and the physical masses

$$\begin{aligned} v^2 \lambda_1 &= m_h^2 - \frac{t_\beta (m_{12}^2 - m_H^2 s_\beta c_\beta)}{c_\beta^2} + (m_h^2 - m_H^2) [c_{\beta-\alpha}^2 (t_\beta^2 - 1) - 2t_\beta s_{\beta-\alpha} c_{\beta-\alpha}], \\ v^2 \lambda_2 &= m_h^2 - \frac{m_{12}^2 - m_H^2 s_\beta c_\beta}{t_\beta s_\beta^2} + (m_h^2 - m_H^2) [c_{\beta-\alpha}^2 (t_\beta^{-2} - 1) + 2t_\beta^{-1} s_{\beta-\alpha} c_{\beta-\alpha}], \\ v^2 \lambda_3 &= m_h^2 + 2m_{H^\pm}^2 - 2m_H^2 - \frac{m_{12}^2 - m_H^2 s_\beta c_\beta}{s_\beta c_\beta} - (m_h^2 - m_H^2) [2c_{\beta-\alpha}^2 + s_{\beta-\alpha} c_{\beta-\alpha} (t_\beta - t_\beta^{-1})], \\ v^2 \lambda_4 &= m_A^2 - 2m_{H^\pm}^2 + m_H^2 - \frac{m_{12}^2 - m_H^2 s_\beta c_\beta}{s_\beta c_\beta}, \\ v^2 \lambda_5 &= m_H^2 - m_A^2 - \frac{m_{12}^2 - m_H^2 s_\beta c_\beta}{s_\beta c_\beta}. \end{aligned} \quad (2.9)$$

We can introduce $\lambda v^2 \equiv m_H^2 - m_{12}^2 / (s_\beta c_\beta)$ following Ref. [44]. The above expression indicates that the unitarity and perturbativity set up upper bounds on the mass splittings, which can be roughly taken as $\lambda v^2 < 4\pi v^2$, $m_A^2 - m_H^2 \lesssim \mathcal{O}(4\pi v^2 - \lambda v^2)$, $m_{H^\pm}^2 - m_H^2 \lesssim \mathcal{O}(4\pi v^2 - \lambda v^2)$ and $\max\{t_\beta, \cot \beta\} \lesssim \sqrt{(8\pi v^2)/(3\lambda v^2)}$. Generally speaking, large mass splitting among non-SM Higgses are not allowed for large values of λv^2 and/or non-SM Higgs masses.

2.3 Direct searches at LEP and LHC

The search for pair-produced charged Higgs bosons at the Large Electron-Positron Collider (LEP) imposes a lower bound of 80 GeV on the mass of the charged Higgs boson [45], and LEP searches for AH production constrain the sum of the masses $m_H + m_A > 209$ GeV [46].

LHC are also looking for direct productions of exotic Higgses via including $A/H \rightarrow \mu\mu$ [47, 48], $A/H \rightarrow bb$ [49, 50], $A/H \rightarrow \tau\tau$ [51–53], $A/H \rightarrow \gamma\gamma$ [54–58], $A/H \rightarrow tt$ [59],

	Current				CEPC				FCC-ee				ILC			
	σ	correlation			σ (10^{-2})	correlation			σ (10^{-2})	correlation			σ (10^{-2})	correlation		
		S	T	U		S	T	U		S	T	U		S	T	U
S	0.04 ± 0.11	1	0.92	-0.68	1.82	1	0.9963	-0.9745	0.370	1	0.9898	-0.8394	2.57	1	0.9947	-0.9431
T	0.09 ± 0.14	-	1	-0.87	2.56	-	1	-0.9844	0.514	-	1	-0.8636	3.59	-	1	-0.9569
U	-0.02 ± 0.11	-	-	1	1.83	-	-	1	0.416	-	-	1	2.64	-	-	1

Table 1. Estimated S , T , and U ranges and correlation matrices ρ_{ij} from Z-pole precision measurements of the current results [78].

$H \rightarrow ZZ$ [60, 61], $H \rightarrow WW$ [62, 63], $A \rightarrow hZ \rightarrow b\bar{b}l\bar{l}$ [64–67], $A \rightarrow hZ \rightarrow \tau\tau\ell\bar{\ell}$ [66, 68, 69], $H \rightarrow hh$ [70–73], and $A/H \rightarrow HZ/AZ$ [74, 75]. The null results have already ruled out a significant portion of parameter space of 2HDM. For a typical mass splitting $m_A - m_H = m_{H^\pm} - m_H = 200$ GeV, the exotic decay channel $A \rightarrow HZ$ has already excluded a neutral Higgs with mass less than $2m_t$ for $\tan\beta < 5$ in Type-I model and for $0.5 < \tan\beta < 15$ in Type-II model. For large $\tan\beta$ region ($\tan\beta > 15$) in Type-II model, this channel put the mass of neutral scalar H to be above 600 GeV. Top quarks search channels, $4t$ and $A/H \rightarrow tt$, rule out $m_H < 800$ GeV for $\tan\beta < 0.3$ and $m_H < 650$ GeV for $\tan\beta < 1.1$ in both two types of 2HDMs. While $A/H \rightarrow \tau\tau, \gamma\gamma$ can exclude the region $m < 350$ GeV, $\tan\beta < 1$ in Type-I and -II models, $A/H \rightarrow \tau\tau$ could fully exclude m_H larger than 800 GeV when $\tan\beta > 10$ in Type-II 2HDM. For a complete recasting the LHC direct search results in the 2HDM, we refer the readers to Ref. [27, 41, 76].

2.4 Z-pole and Higgs precision measurements

Measurements of Z-pole observables at the Large Electron-Positron Collider (LEP) impose strong constraints on the 2HDM [77]. Satisfying Z-pole constraints requires the charged scalar mass to be close to one of the heavy neutral scalar masses: $m_{H^\pm} \simeq m_H$ or $m_{H^\pm} \simeq m_A$. In our analysis, we simply take the S, T, U data at 95% Confidence Level (C.L.) in Tab. 1 to capture the dominant contributions from Z-pole measurements. Note that a global analysis to recast the S, T, U parameters is needed by including both Z-pole observables and latest W mass measurement [3], here for simplicity we just take them as two separate measurements and are going to discuss more on the W boson mass effects in Sec. 2.5.

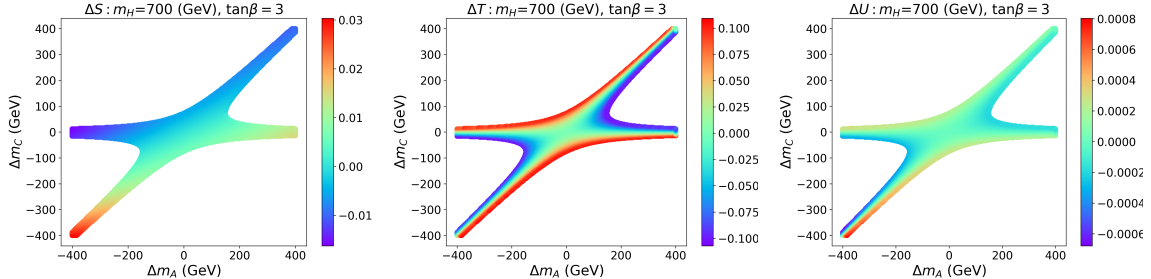


Figure 1. Current oblique constraints S, T, U in the plane of $\Delta m_A - \Delta m_C$ with $m_H = 700$ GeV, $\tan\beta = 3$ in the alignment limit $\cos(\beta - \alpha) = 0$. The colors are for corresponding parameter value.

To reveal the relation between non-SM Higgs spectra and S, T, U , we define following mass splitting parameters:

$$\Delta m_A = m_A - m_H, \Delta m_C = m_{H^\pm} - m_H \quad (2.10)$$

In [Fig. 1](#) we present the S, T, U deviation from their SM value as functions of Δm_A and Δm_C . Current measure uncertainty for S, T, U are around 10%, so it can be seen that T parameter provides the most stringent limit on non-SM Higgs mass splitting.

The LHC has also performed high precision tests on the Higgs couplings, which indicates all the measurable couplings κ_i are close to their SM values. Future Higgs factories will further improve the precision of measurements in the Higgs sector, and we therefore include hypothetical future lepton collider results in our study. We adopt the Higgs measurements results presented in Table 3 in Ref. [\[79\]](#). Note that for future experiments, we assume there is no deviation from the SM in Higgs measurements.

2.5 m_W in the 2HDM

As an important observable used in the SM precise test, m_W is closely related to Z boson mass m_Z , Fermi constant G_F , and fine structure constant α

$$m_W^2 \left(1 - \frac{m_W^2}{m_Z^2} \right) = \frac{\pi\alpha}{\sqrt{2}G_F} (1 + \Delta r) \quad (2.11)$$

where Δr corresponds to quantum corrections [\[35\]](#). In the 2HDM, m_W correction can be represented by [\[80\]](#)

$$m_W^{2\text{HDM}} = m_W^{\text{SM}} \left[1 + \frac{\alpha c_W^2}{2(c_W^2 - s_W^2)} T (1 + \delta\rho^{2\text{HDM}}) + \frac{\alpha}{8s_W^2} U - \frac{\alpha}{4(c_W^2 - s_W^2)} S \right] \quad (2.12)$$

to the $\mathcal{O}(\alpha^2)$. Here $m_W^{\text{SM}} = 80.357 \text{ GeV} \pm 4_{\text{inputs}} \pm 4_{\text{theory}} \text{ MeV}$ [\[3\]](#), S, T, U are oblique parameters in the 2HDM [\[78\]](#), and $\delta\rho^{2\text{HDM}} = \frac{|\lambda_{hhh}^{2\text{HDM}}|^2}{16\pi^2 m_h^2}$ are higher order 2HDM effects from enhanced Higgs boson self-interactions. Currently $\kappa_{hhh} = \lambda_{hhh}^{2\text{HDM}}/\lambda_{hhh}^{\text{SM}} \in (-1.0, 6.6)$ [\[81\]](#) is already strongly constrained, thus the higher order effect $\delta\rho^{2\text{HDM}}$ up to $\mathcal{O}(0.01)$ is weak.

For convenient, we define

$$\Delta m_W^{2\text{HDM}} = m_W^{2\text{HDM}} - m_W^{\text{SM}} \quad (2.13)$$

In the left panel of [Fig. 2](#) where we take $\Delta U = 0$ as a benchmark case, we show the general picture of $\Delta m_W^{2\text{HDM}}$ in the plane of $\Delta T - \Delta S$ based on the allowed region shown in the [Fig. 1](#). The colors show values of $\Delta m_W^{2\text{HDM}}$, varying from -50 MeV to 50 MeV. We have 5 black dash-dotted lines for $\Delta m_W^{2\text{HDM}} = -40, -20, 0, 20, \text{ and } 40 \text{ MeV}$. Generally speaking, $\Delta m_W^{2\text{HDM}}$ mainly depends on ΔT , and the larger ΔT and smaller ΔS result in large $\Delta m_W^{2\text{HDM}}$. This result can be easily understood with the sizes of the coefficients in front of S, T, U in [Eq. \(2.12\)](#). In the right panel, we take the benchmark spectrum of [Fig. 1](#) with $m_H = 700 \text{ GeV}$ and

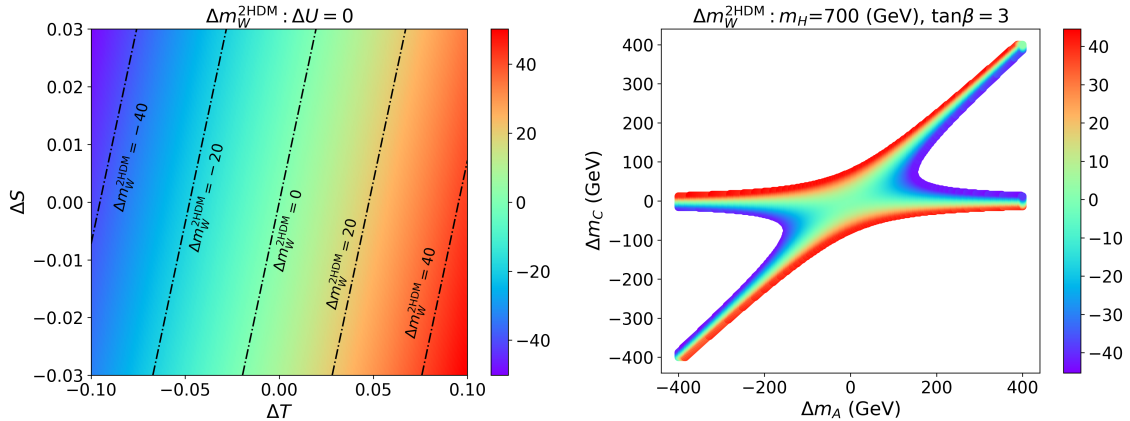


Figure 2. (Left): general picture of $\Delta m_W^{2\text{HDM}}$ in the plane of $\Delta T - \Delta S$ with $\Delta U = 0$. The colors are values of $\Delta m_W^{2\text{HDM}}$, varying from -50 MeV to 50 MeV. We have 5 black dash-dotted lines for $\Delta m_W^{2\text{HDM}} = -40, -20, 0, 20,$ and 40 MeV. (Right): $m_W^{2\text{HDM}}$ in the plane of $\Delta m_A - \Delta m_C$ with same benchmark spectrum $m_H = 700$ GeV as Fig. 1. The colors are same to the left panel.

$\tan\beta = 3$, and show $\Delta m_W^{2\text{HDM}}$ in the plane of $\Delta m_A - \Delta m_C$. We can see that, under current various constraints, the benchmark spectrum here can supply for the theoretical correction meeting the new experimental measurement at CDF-II [3]. Since in the 2HDM, $\Delta m_W^{2\text{HDM}}$ is directly relevant to oblique parameters, and oblique parameters further depend on non-SM Higgs mass splitting Δm_A and Δm_C . So it is clear that $\Delta m_W^{2\text{HDM}}$ is sensitive to non-SM Higgs mass splitting.

2.6 Flavour constraints

The charged Higgs H^\pm boson couples to both up and down type fermions, which can lead to flavor changing processes strongly constrained by flavor physics observations. The most stringent of limits comes from the measurements of B-meson decays (e.g. $b \rightarrow s\gamma$ and $B^+ \rightarrow \tau\nu$), which disfavor $m_{H^\pm} < 580$ GeV and large values of $\tan\beta$ respectively in Type-II 2HDM [82, 83], or $m_{H^\pm} < 1$ TeV and small values of $\tan\beta$ ($\tan\beta < 1$) in Type-I model [83]. However, flavor constraints can be alleviated with contributions from other sectors of the BSM models [84]. In this paper, we only focus on the constraints from B-physics on the scalar sector.

2.7 Phase transition in the 2HDM

To study EWPT, we need to know the thermal effective potential, which is the free-energy density, as the function of scalar VEVs. The thermal effective potential $V(\phi_1, \phi_2, T)$ can be schematically expressed as:

$$V(\phi_1, \phi_2, T) = V^0(\phi_1, \phi_2) + V^{\text{CW}}(\phi_1, \phi_2) + V^{\text{CT}}(\phi_1, \phi_2) + V^{\text{T}}(\phi_1, \phi_2, T). \quad (2.14)$$

Here ϕ_i are scalar VEVs, T is the temperature of thermal system, $V^0(\phi_1, \phi_2)$ is the tree-level potential, $V^{\text{CW}}(\phi_1, \phi_2)$ and $V^{\text{CT}}(\phi_1, \phi_2)$ are Coleman-Weinberg potential and counter term respectively, and $V^{\text{T}}(\phi_1, \phi_2, T)$ is thermal correction. Detailed formulas can be found in the literature [25, 26].

In the very early universe, temperature T is much higher than all the particles' mass in our model. The large effective thermal mass keep ϕ_i at zero and thus maintain the EW-symmetry. And when T become much lower than EW scale, the global minimum position of $V(\phi_1, \phi_2, T)$ on $\phi_1 - \phi_2$ plane must move to a place where $\phi_1^2 + \phi_2^2 \neq 0$ to break EW-symmetry. To know whether this phase transition process is first-order, we can track the minimum point with T decreasing. If the minimum point (which locates in zero point when T is very large) “jump to” a non-zero point discontinuously at critical temperature T_c , then the EWPT should be first-order. This method has been numerically implemented in public package `BSMPT` [85]. We will use this package in this work.

Furthermore, to prevent baryon number being washed out inside Higgs bubble, the “wash out” parameter [24] $\xi_c \equiv v_c/T_c$ (v_c is the Higgs VEV at T_c) should roughly be larger than 1. Considering the uncertainty in ξ_c calculation [28, 29], we use a slightly looser criteria for SFOEWPT:

$$\xi_c \equiv \frac{v_c}{T_c} > 0.9 \quad (2.15)$$

3 Study results

In this section, we try to explore the SFOEWPT under various current and future constraints. Specially we have a detailed study about the latest m_W result at CDF-II.

We will firstly have a large amount of random scan points, and our study include the theoretical constraints, B -physics, LHC Run-II direct searches, current precision measurement of Higgs and Z-pole physics. Then the further study is performed at future Higgs factories, including CEPC, FCC-ee and ILC as shown in [Tab. 1](#), to confront the SFOEWPT and m_W anomaly. Our study of Higgs precision measurements will deep into one-loop level.

3.1 Study method

We perform a 6 parameters random scan for both Type-I and Type-II, and the scan regions are :

$$\begin{aligned} \tan \beta \in (0.2, 50), |\cos(\beta - \alpha)| < 0.5, m_{A/H^\pm} \in (10, 1500) \text{ GeV} , \\ m_{12}^2 \in (0, 1500^2) \text{ GeV}^2, m_H \in (130, 1500) \text{ GeV}. \end{aligned} \quad (3.1)$$

The number of samples allowed by current various (except for m_W from CDF-II) is more than 1 million (of 1 billion points in total) . After considering the SFOEWPT, it is about a few hundreds of thousands points allowed for Type-I, but much less for Type-II to be shown in [Fig. 3](#) as grey dots.

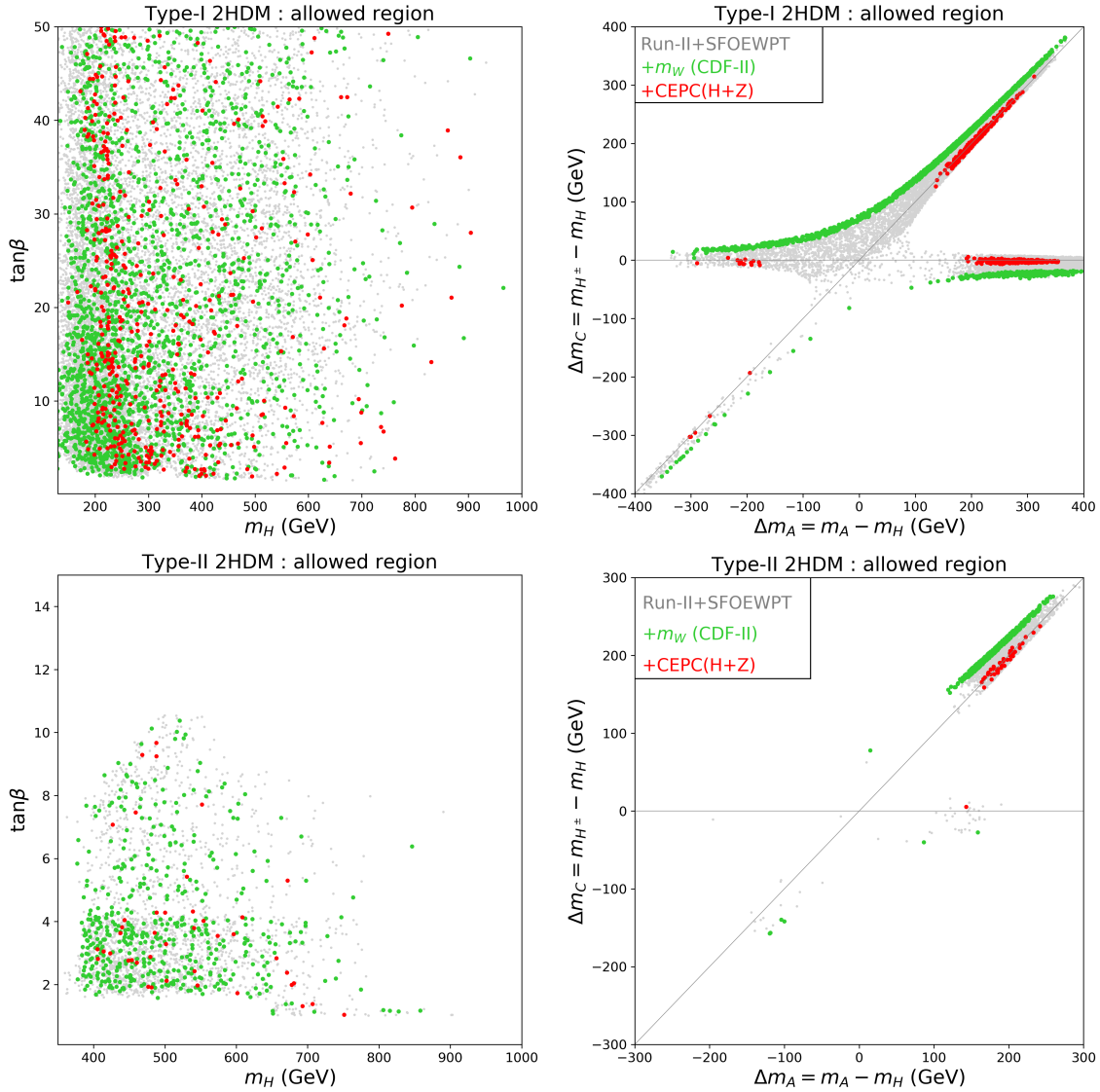


Figure 3. The allowed parameter space in the plane of $m_H - \tan\beta$ (left), $\Delta m_A - \Delta m_C$ (right). The grey points survive all theoretical constraints, current experimental constraints, and the conditions of SFOEWPT. The top and bottom panels are for Type-I and Type-II respectively. The green ones are able to provide a m_W by CDF-II, while the red ones are allowed by future Higgs and Z-pole precision measurements from CEPC. The red and green points do not cover each other.

To incorporate in the m_W at CDF-II, here in the 2HDM based on Eq. (2.12), we take the m_W data at 95% Confidence Level (C.L.) with the χ^2 profile-likelihood fit,

$$\chi^2 = \frac{(m_W^{2\text{HDM}} - m_W^{\text{obs}})^2}{\sum \sigma_{m_W}^2}, \quad (3.2)$$

After taking into account of experiment uncertainties, we have

$$\Delta m_W^{2\text{HDM}}|_{\text{ex}} \in (36.3, 103.4) \text{ MeV}, \quad (3.3)$$

and if considering SM theoretical uncertainties as well, it is $\Delta m_W^{2\text{HDM}}|_{\text{th+ex}} \in (31.1, 108.9) \text{ MeV}$ for the 6 parameter scan at 95% C.L.. We will only take $\Delta m_W^{2\text{HDM}}|_{\text{ex}}$ as condition of m_W for CDF-II in the following study².

3.2 SFOEWPT under LHC measurements

As discussed above, after scanning the entire parameter space of Type-I and Type-II 2HDM, we obtain the sector which is allowed by current limits and also satisfy the SFOEWPT requirement.

As shown in Fig. 3, the grey points meet all the conditions of current various measurements(except for m_W at CDF-II) and SFOEWPT inboth types. For Type-I and Type-II, favored mass region are different:

- Type-I: To satisfy SFOEWPT and current limits, m_H distributes in region (125, 1000) GeV with $\tan \beta$ varying from 1 to 50. Mass splitting $m_{H^\pm} - m_H$ and $m_A - m_H$ distribute in region $(-400, 400) \text{ GeV}$.
- Type-II: Compared with Type-I, Type-II is more limited due to the limited $\tan \beta$ region. m_H distributes in region (125, 1000) GeV, while $\tan \beta$ is limited to (1, 12). Mass splitting $m_{H^\pm} - m_H$ and $m_A - m_H$ vary in region $(-200, 300) \text{ GeV}$.

To summarize, SFOEWPT require the mass of non-SM Higgs $H/A/H^\pm$ to be smaller than 1 TeV and a certain amount of splitting between them. Comparing with the right panel of Fig. 2, it is clear that the uplifted m_W is consistent with SFOEWPT requirement.

3.3 SFOEWPT under Higgs, Z and W precision measurements

As discussed above, SFOEWPT, Higgs precision measurements at one-loop level, and Z-pole physics (oblique parameter S, T, U) are all connected by heavy Higgs mass splitting. In more detail, Fig. 2 and Eq. (2.12) tells that non-zero $\Delta S/T$ is needed for uplifting m_W . But Higgs and Z-pole physics have strong constraints on the value of $\Delta S/T$. As presented in Fig. 3, the green points meets all these Higgs, Z-pole, m_W and SFOEWPT conditions. Compared to the grey points, we can see the allowed $\tan \beta, m_H, \Delta m_A$ and Δm_C region of green points does not change a lot. Another feature is they mainly locate around the boundary region, which is mainly because current electroweak measurements is not precise enough, so the uplifted m_W in need can still be satisfied within 2HDM framework. As shown in our benchmark case Fig. 1, specific ΔT is in need. Since oblique parameters is type universal, thus Type-I and Type-II have similar features for green region.

However, future lepton colliders, such as CEPC, ILC, and FCC-ee, will measure electroweak parameters to unprecedented precision. As presented in Tab. 1, uncertainties of

²There is no apparent difference found for $\Delta m_W^{2\text{HDM}}|_{\text{ex}}$ and $\Delta m_W^{2\text{HDM}}|_{\text{th+ex}}$ in our study.

oblique measurements in CEPC can be reduced to 1% level, which one order smaller than current uncertainties. For the Higgs precision measurements, the works [44, 78, 79] have discussed them for the case of 2HDM systematically. Provided that there is no apparent deviation of Higgs and Z-pole proprieties to the SM predictions observed, or in other words, the future measurements turn out to be consistent with SM prediction, we take CEPC precision measurements as an example to study the impact from future lepton colliders. Finally as shown in Fig. 3, the red points represent spectrum meeting conditions of Higgs, Z-pole measurements, and SFOEWPT. We can see, the red region is strongly restricted to $\Delta m_A = 0$ or $\Delta m_C = \Delta m_A$ for both types. For Type-I, it is $\Delta m_C = \Delta m_A, |\Delta m_A| \in (150, 350)\text{GeV}$, or $\Delta m_C = 0, |\Delta m_A| \in (150, 350)\text{GeV}$. While for Type-II, it is $\Delta m_C = \Delta m_A$ and $\Delta m_A \in (150, 250)\text{GeV}$. In both types, the red region and green region are separate from each other, which means Higgs+Z-pole measurements at CEPC can exclude the region for m_W at CDF-II.

On the other hand, if SFOEWPT with uplifted m_W in 2HDM is the true BSM scenario, deviations from SM prediction will be observed at future measurements with high confidence level.

4 Conclusion

In this work, we revisited the existence of a strong first order electroweak phase transition (SFOEWPT) in the Type-I and Type-II 2HDMs as the grey points in Fig. 3. At the same time, the latest precision measurement of the m_W at CDF-II, indicates possible existence of new particles with mass around electroweak scale. We studied them all in the framework of 2HDM.

In detail, we carried out a global analysis, including W boson mass m_W , SFOEWPT requirements, direct searches of scalar resonances at the LHC, and current LHC and future Higgs and Z-pole precision measurements at lepton colliders such as CEPC, ILC, FCC-ee. We found that,

1. Since in the 2HDM, $\Delta m_W^{2\text{HDM}}$ is directly relevant to oblique parameters as discussed, which is dependent on the heavy Higgs mass splitting of $\Delta m_A = m_A - m_H$ and $\Delta m_C = m_{H^\pm} - m_H$, we can see $\Delta m_W^{2\text{HDM}}$ is sensitive to heavy Higgs mass splitting. As a result, all these precision measurements and SFOEWPT in 2HDM are sensitive to non-SM Higgs mass splitting in 2HDM.
2. Under current constraints, both Type-I and Type-II 2HDM can explain the SFOEWPT, Z-pole, Higgs precision measurements and m_W precision measurement of CDF-II at same time. In the Fig. 3, we have the green points satisfying all of them, under current various constraints. Generally the allowed region are

$$m_H \in (125, 950) \text{ GeV}, \Delta m_{A/C} \in (-400, 400) \text{ GeV}, \tan \beta \in (1, 50)$$

for Type-I,

$$m_H \in (125, 900) \text{ GeV}, \Delta m_{A/C} \in (-200, 300) \text{ GeV}, \tan \beta \in (1, 12)$$

for Type-II.

3. With future precision measurements at CEPC, ILC, or FCC-ee, if there is no deviation to SM observed at Higgs or Z-pole physics, SFOEWPT is still allowed, but m_W from CDF-II can not explained anymore by 2HDM. In other words, if 2HDM is the true BSM scenario after lepton colliders run, deviations from SM prediction will be observed at future measurements with high confidence level.

Such a constrained parameter space points out a clear direction for experimental studies and also theoretical explorations for explaining other phenomenology.

Acknowledgments

We thank Jin Min Yang, Shufang Su, Yang Zhang for useful discussions and comments. H.S. is supported by the International Postdoctoral Exchange Fellowship Program. W.S. is supported by KIAS Individual Grant (PG084201) at Korea Institute for Advanced Study. M.Z. was supported by the National Natural Science Foundation of China (NNSFC) under Grant No. 12105118 and 11947118.

References

- [1] **ATLAS** Collaboration, G. Aad et al., *Observation of a new particle in the search for the Standard Model Higgs boson with the ATLAS detector at the LHC*, *Phys. Lett.* **B716** (2012) 1–29, [[arXiv:1207.7214](#)].
- [2] **CMS** Collaboration, S. Chatrchyan et al., *Observation of a new boson at a mass of 125 GeV with the CMS experiment at the LHC*, *Phys. Lett.* **B716** (2012) 30–61, [[arXiv:1207.7235](#)].
- [3] **CDF** Collaboration, T. Aaltonen et al., *High-precision measurement of the W boson mass with the CDF II detector*, *Science* **376** (2022), no. 6589 170–176.
- [4] Y.-Z. Fan, T.-P. Tang, Y.-L. S. Tsai, and L. Wu, *Inert Higgs Dark Matter for New CDF W-boson Mass and Detection Prospects*, [arXiv:2204.03693](#).
- [5] C.-T. Lu, L. Wu, Y. Wu, and B. Zhu, *Electroweak Precision Fit and New Physics in light of W Boson Mass*, [arXiv:2204.03796](#).
- [6] P. Athron, A. Fowlie, C.-T. Lu, L. Wu, Y. Wu, and B. Zhu, *The W boson Mass and Muon $g - 2$: Hadronic Uncertainties or New Physics?*, [arXiv:2204.03996](#).
- [7] G.-W. Yuan, L. Zu, L. Feng, and Y.-F. Cai, *W-boson mass anomaly: probing the models of axion-like particle, dark photon and Chameleon dark energy*, [arXiv:2204.04183](#).
- [8] A. Strumia, *Interpreting electroweak precision data including the W-mass CDF anomaly*, [arXiv:2204.04191](#).
- [9] J. M. Yang and Y. Zhang, *Low energy SUSY confronted with new measurements of W-boson mass and muon $g-2$* , [arXiv:2204.04202](#).
- [10] J. de Blas, M. Pierini, L. Reina, and L. Silvestrini, *Impact of the recent measurements of the top-quark and W-boson masses on electroweak precision fits*, [arXiv:2204.04204](#).

- [11] C.-R. Zhu, M.-Y. Cui, Z.-Q. Xia, Z.-H. Yu, X. Huang, Q. Yuan, and Y. Z. Fan, *GeV antiproton/gamma-ray excesses and the W-boson mass anomaly: three faces of $\sim 60 - 70$ GeV dark matter particle?*, [arXiv:2204.03767](#).
- [12] J. M. Cline, *Baryogenesis*, in *Les Houches Summer School - Session 86: Particle Physics and Cosmology: The Fabric of Spacetime*, 9, 2006. [hep-ph/0609145](#).
- [13] D. E. Morrissey and M. J. Ramsey-Musolf, *Electroweak baryogenesis*, *New J. Phys.* **14** (2012) 125003, [[arXiv:1206.2942](#)].
- [14] N. S. Manton, *Topology in the Weinberg-Salam Theory*, *Phys. Rev. D* **28** (1983) 2019.
- [15] F. R. Klinkhamer and N. S. Manton, *A Saddle Point Solution in the Weinberg-Salam Theory*, *Phys. Rev. D* **30** (1984) 2212.
- [16] V. A. Kuzmin, V. A. Rubakov, and M. E. Shaposhnikov, *On the Anomalous Electroweak Baryon Number Nonconservation in the Early Universe*, *Phys. Lett. B* **155** (1985) 36.
- [17] K. Kajantie, M. Laine, K. Rummukainen, and M. E. Shaposhnikov, *Is there a hot electroweak phase transition at $m(H)$ larger or equal to $m(W)$?*, *Phys. Rev. Lett.* **77** (1996) 2887–2890, [[hep-ph/9605288](#)].
- [18] F. Csikor, Z. Fodor, and J. Heitger, *Endpoint of the hot electroweak phase transition*, *Phys. Rev. Lett.* **82** (1999) 21–24, [[hep-ph/9809291](#)].
- [19] M. Carena, Z. Liu, and M. Riembau, *Probing the electroweak phase transition via enhanced di-Higgs boson production*, *Phys. Rev. D* **97** (2018), no. 9 095032, [[arXiv:1801.00794](#)].
- [20] J. M. Cline and K. Kainulainen, *Electroweak baryogenesis and dark matter from a singlet Higgs*, *JCAP* **01** (2013) 012, [[arXiv:1210.4196](#)].
- [21] J. M. Cline, K. Kainulainen, and D. Tucker-Smith, *Electroweak baryogenesis from a dark sector*, *Phys. Rev. D* **95** (2017), no. 11 115006, [[arXiv:1702.08909](#)].
- [22] M. Carena, M. Quirós, and Y. Zhang, *Electroweak Baryogenesis from Dark-Sector CP Violation*, *Phys. Rev. Lett.* **122** (2019), no. 20 201802, [[arXiv:1811.09719](#)].
- [23] J. M. Cline, G. Laporte, H. Yamashita, and S. Kraml, *Electroweak Phase Transition and LHC Signatures in the Singlet Majoron Model*, *JHEP* **07** (2009) 040, [[arXiv:0905.2559](#)].
- [24] G. D. Moore, *Measuring the broken phase sphaleron rate nonperturbatively*, *Phys. Rev. D* **59** (1999) 014503, [[hep-ph/9805264](#)].
- [25] S. R. Coleman and E. J. Weinberg, *Radiative Corrections as the Origin of Spontaneous Symmetry Breaking*, *Phys. Rev. D* **7** (1973) 1888–1910.
- [26] P. B. Arnold and O. Espinosa, *The Effective potential and first order phase transitions: Beyond leading-order*, *Phys. Rev. D* **47** (1993) 3546, [[hep-ph/9212235](#)]. [Erratum: *Phys. Rev. D* 50, 6662 (1994)].
- [27] W. Su, A. G. Williams, and M. Zhang, *Strong first order electroweak phase transition in 2HDM confronting future Z & Higgs factories*, *JHEP* **04** (2021) 219, [[arXiv:2011.04540](#)].
- [28] N. Nielsen, *On the Gauge Dependence of Spontaneous Symmetry Breaking in Gauge Theories*, *Nucl. Phys. B* **101** (1975) 173–188.

- [29] K. Kainulainen, V. Keus, L. Niemi, K. Rummukainen, T. V. Tenkanen, and V. Vaskonen, *On the validity of perturbative studies of the electroweak phase transition in the Two Higgs Doublet model*, *JHEP* **06** (2019) 075, [[arXiv:1904.01329](#)].
- [30] F. P. Huang and C. S. Li, *Electroweak baryogenesis in the framework of the effective field theory*, *Phys. Rev. D* **92** (2015), no. 7 075014, [[arXiv:1507.08168](#)].
- [31] F. P. Huang, Z. Qian, and M. Zhang, *Exploring dynamical CP violation induced baryogenesis by gravitational waves and colliders*, *Phys. Rev. D* **98** (2018), no. 1 015014, [[arXiv:1804.06813](#)].
- [32] D. López-Val and T. Robens, *Δr and the W -boson mass in the singlet extension of the standard model*, *Phys. Rev. D* **90** (2014) 114018, [[arXiv:1406.1043](#)].
- [33] T. Lee, *A Theory of Spontaneous T Violation*, *Phys. Rev. D* **8** (1973) 1226–1239.
- [34] G. C. Branco, P. M. Ferreira, L. Lavoura, M. N. Rebelo, M. Sher, and J. P. Silva, *Theory and phenomenology of two-Higgs-doublet models*, *Phys. Rept.* **516** (2012) 1–102, [[arXiv:1106.0034](#)].
- [35] D. Lopez-Val and J. Sola, *Delta r in the Two-Higgs-Doublet Model at full one loop level – and beyond*, *Eur. Phys. J. C* **73** (2013) 2393, [[arXiv:1211.0311](#)].
- [36] P. Bambade et al., *The International Linear Collider: A Global Project*, [arXiv:1903.01629](#).
- [37] **FCC Collaboration**, A. Abada et al., *FCC Physics Opportunities: Future Circular Collider Conceptual Design Report Volume 1*, *Eur. Phys. J. C* **79** (2019), no. 6 474.
- [38] **FCC Collaboration**, A. Abada et al., *FCC-ee: The Lepton Collider: Future Circular Collider Conceptual Design Report Volume 2*, *Eur. Phys. J. ST* **228** (2019), no. 2 261–623.
- [39] **CEPC Study Group** Collaboration, M. Dong et al., *CEPC Conceptual Design Report: Volume 2 - Physics & Detector*, [arXiv:1811.10545](#).
- [40] **CEPC Physics-Detector Study Group** Collaboration, *The CEPC input for the European Strategy for Particle Physics - Physics and Detector*, [arXiv:1901.03170](#).
- [41] L. Wang, J. M. Yang, and Y. Zhang, *Two-Higgs-doublet models in light of current experiments: a brief review*, [arXiv:2203.07244](#).
- [42] J. F. Gunion and H. E. Haber, *The CP conserving two Higgs doublet model: The Approach to the decoupling limit*, *Phys. Rev. D* **67** (2003) 075019, [[hep-ph/0207010](#)].
- [43] I. F. Ginzburg and I. P. Ivanov, *Tree-level unitarity constraints in the most general 2HDM*, *Phys. Rev. D* **72** (2005) 115010, [[hep-ph/0508020](#)].
- [44] J. Gu, H. Li, Z. Liu, S. Su, and W. Su, *Learning from Higgs Physics at Future Higgs Factories*, *JHEP* **12** (2017) 153, [[arXiv:1709.06103](#)].
- [45] **ALEPH, DELPHI, L3, OPAL, LEP** Collaboration, G. Abbiendi et al., *Search for Charged Higgs bosons: Combined Results Using LEP Data*, *Eur. Phys. J. C* **73** (2013) 2463, [[arXiv:1301.6065](#)].
- [46] **ALEPH, DELPHI, L3, OPAL, LEP Working Group for Higgs Boson Searches** Collaboration, S. Schael et al., *Search for neutral MSSM Higgs bosons at LEP*, *Eur. Phys. J. C* **47** (2006) 547–587, [[hep-ex/0602042](#)].
- [47] **CMS** Collaboration, A. M. Sirunyan et al., *Search for MSSM Higgs bosons decaying to $\mu^+\mu^-$*

- in proton-proton collisions at $\sqrt{s} = 13$ TeV Search for MSSM Higgs bosons decaying to $\mu^+\mu^-$ in proton-proton collisions at $s=13$ TeV, *Phys. Lett.* **B798** (2019) 134992, [[arXiv:1907.03152](#)].
- [48] **ATLAS** Collaboration, M. Aaboud et al., Search for scalar resonances decaying into $\mu^+\mu^-$ in events with and without b -tagged jets produced in proton-proton collisions at $\sqrt{s} = 13$ TeV with the ATLAS detector, *JHEP* **07** (2019) 117, [[arXiv:1901.08144](#)].
- [49] **CMS** Collaboration, A. M. Sirunyan et al., Search for beyond the standard model Higgs bosons decaying into a $b\bar{b}$ pair in pp collisions at $\sqrt{s} = 13$ TeV, *JHEP* **08** (2018) 113, [[arXiv:1805.12191](#)].
- [50] **ATLAS** Collaboration, G. Aad et al., Search for heavy neutral Higgs bosons produced in association with b -quarks and decaying to b -quarks at $\sqrt{s} = 13$ TeV with the ATLAS detector, [arXiv:1907.02749](#).
- [51] **CMS** Collaboration, A. M. Sirunyan et al., Search for additional neutral MSSM Higgs bosons in the $\tau\tau$ final state in proton-proton collisions at $\sqrt{s} = 13$ TeV, *JHEP* **09** (2018) 007, [[arXiv:1803.06553](#)].
- [52] **CMS** Collaboration, A. M. Sirunyan et al., Search for a low-mass $\tau^+\tau^-$ resonance in association with a bottom quark in proton-proton collisions at $\sqrt{s} = 13$ TeV, *JHEP* **05** (2019) 210, [[arXiv:1903.10228](#)].
- [53] **ATLAS** Collaboration, G. Aad et al., Search for heavy Higgs bosons decaying into two tau leptons with the ATLAS detector using pp collisions at $\sqrt{s} = 13$ TeV, [arXiv:2002.12223](#).
- [54] **CMS** Collaboration, A. M. Sirunyan et al., Search for a standard model-like Higgs boson in the mass range between 70 and 110 GeV in the diphoton final state in proton-proton collisions at $\sqrt{s} = 8$ and 13 TeV, *Phys. Lett.* **B793** (2019) 320–347, [[arXiv:1811.08459](#)].
- [55] **CMS** Collaboration, A. M. Sirunyan et al., Search for physics beyond the standard model in high-mass diphoton events from proton-proton collisions at $\sqrt{s} = 13$ TeV, *Phys. Rev.* **D98** (2018), no. 9 092001, [[arXiv:1809.00327](#)].
- [56] **ATLAS** Collaboration, G. Aad et al., Search for Scalar Diphoton Resonances in the Mass Range 65 – 600 GeV with the ATLAS Detector in pp Collision Data at $\sqrt{s} = 8$ TeV, *Phys. Rev. Lett.* **113** (2014), no. 17 171801, [[arXiv:1407.6583](#)].
- [57] **ATLAS** Collaboration, M. Aaboud et al., Search for new phenomena in high-mass diphoton final states using 37 fb^{-1} of proton-proton collisions collected at $\sqrt{s} = 13$ TeV with the ATLAS detector, *Phys. Lett.* **B775** (2017) 105–125, [[arXiv:1707.04147](#)].
- [58] **ATLAS** Collaboration, T. A. collaboration, Search for resonances in the 65 to 110 GeV diphoton invariant mass range using 80 fb^{-1} of pp collisions collected at $\sqrt{s} = 13$ TeV with the ATLAS detector, .
- [59] **CMS** Collaboration, A. M. Sirunyan et al., Search for heavy Higgs bosons decaying to a top quark pair in proton-proton collisions at $\sqrt{s} = 13$ TeV, [arXiv:1908.01115](#).
- [60] **CMS** Collaboration, A. M. Sirunyan et al., Search for a new scalar resonance decaying to a pair of Z bosons in proton-proton collisions at $\sqrt{s} = 13$ TeV, *JHEP* **06** (2018) 127, [[arXiv:1804.01939](#)]. [Erratum: *JHEP*03,128(2019)].
- [61] **ATLAS** Collaboration, M. Aaboud et al., Search for heavy ZZ resonances in the $\ell^+\ell^-\ell^+\ell^-$ and

- $\ell^+\ell^-\nu\bar{\nu}$ final states using proton–proton collisions at $\sqrt{s} = 13$ TeV with the ATLAS detector, *Eur. Phys. J.* **C78** (2018), no. 4 293, [[arXiv:1712.06386](#)].
- [62] **CMS** Collaboration, A. M. Sirunyan et al., *Search for a heavy Higgs boson decaying to a pair of W bosons in proton–proton collisions at $\sqrt{s} = 13$ TeV*, [arXiv:1912.01594](#).
- [63] **ATLAS** Collaboration, M. Aaboud et al., *Search for heavy resonances decaying into WW in the $e\nu\mu\nu$ final state in pp collisions at $\sqrt{s} = 13$ TeV with the ATLAS detector*, *Eur. Phys. J.* **C78** (2018), no. 1 24, [[arXiv:1710.01123](#)].
- [64] **CMS** Collaboration, V. Khachatryan et al., *Search for a pseudoscalar boson decaying into a Z boson and the 125 GeV Higgs boson in $llbb$ final states*, *Phys. Lett.* **B748** (2015) 221–243, [[arXiv:1504.04710](#)].
- [65] **CMS** Collaboration, A. M. Sirunyan et al., *Search for a heavy pseudoscalar boson decaying to a Z and a Higgs boson at $\sqrt{s} = 13$ TeV*, *Eur. Phys. J.* **C79** (2019), no. 7 564, [[arXiv:1903.00941](#)].
- [66] **ATLAS** Collaboration, G. Aad et al., *Search for a CP-odd Higgs boson decaying to Zh in pp collisions at $\sqrt{s} = 8$ TeV with the ATLAS detector*, *Phys. Lett.* **B744** (2015) 163–183, [[arXiv:1502.04478](#)].
- [67] **ATLAS** Collaboration, M. Aaboud et al., *Search for heavy resonances decaying into a W or Z boson and a Higgs boson in final states with leptons and b -jets in 36 fb^{-1} of $\sqrt{s} = 13$ TeV pp collisions with the ATLAS detector*, *JHEP* **03** (2018) 174, [[arXiv:1712.06518](#)]. [Erratum: *JHEP*11,051(2018)].
- [68] **CMS** Collaboration, V. Khachatryan et al., *Searches for a heavy scalar boson H decaying to a pair of 125 GeV Higgs bosons hh or for a heavy pseudoscalar boson A decaying to Zh , in the final states with $h \rightarrow \tau\tau$* , *Phys. Lett.* **B755** (2016) 217–244, [[arXiv:1510.01181](#)].
- [69] **CMS** Collaboration, A. M. Sirunyan et al., *Search for a heavy pseudoscalar Higgs boson decaying into a 125 GeV Higgs boson and a Z boson in final states with two tau and two light leptons at $\sqrt{s} = 13$ TeV*, [arXiv:1910.11634](#).
- [70] **CMS** Collaboration, A. M. Sirunyan et al., *Search for Higgs boson pair production in the $bb\tau\tau$ final state in proton–proton collisions at $\sqrt{s} = 8$ TeV*, *Phys. Rev.* **D96** (2017), no. 7 072004, [[arXiv:1707.00350](#)].
- [71] **CMS** Collaboration, A. M. Sirunyan et al., *Combination of searches for Higgs boson pair production in proton–proton collisions at $\sqrt{s} = 13$ TeV*, *Phys. Rev. Lett.* **122** (2019), no. 12 121803, [[arXiv:1811.09689](#)].
- [72] **ATLAS** Collaboration, G. Aad et al., *Searches for Higgs boson pair production in the $hh \rightarrow bb\tau\tau, \gamma\gamma WW^*, \gamma\gamma bb, bbbb$ channels with the ATLAS detector*, *Phys. Rev.* **D92** (2015) 092004, [[arXiv:1509.04670](#)].
- [73] **ATLAS** Collaboration, G. Aad et al., *Combination of searches for Higgs boson pairs in pp collisions at $\sqrt{s} = 13$ TeV with the ATLAS detector*, [arXiv:1906.02025](#).
- [74] **ATLAS** Collaboration, M. Aaboud et al., *Search for a heavy Higgs boson decaying into a Z boson and another heavy Higgs boson in the $llbb$ final state in pp collisions at $\sqrt{s} = 13$ TeV with the ATLAS detector*, *Phys. Lett.* **B783** (2018) 392–414, [[arXiv:1804.01126](#)].

- [75] **CMS** Collaboration, A. M. Sirunyan et al., *Search for new neutral Higgs bosons through the $H \rightarrow ZA \rightarrow \ell^+ \ell^- b\bar{b}$ process in pp collisions at $\sqrt{s} = 13$ TeV*, [arXiv:1911.03781](#).
- [76] F. Kling, S. Su, and W. Su, *2HDM Neutral Scalars under the LHC*, *JHEP* **06** (2020) 163, [[arXiv:2004.04172](#)].
- [77] **ALEPH, DELPHI, L3, OPAL, SLD, LEP Electroweak Working Group, SLD Electroweak Group, SLD Heavy Flavour Group** Collaboration, S. Schael et al., *Precision electroweak measurements on the Z resonance*, *Phys. Rept.* **427** (2006) 257–454, [[hep-ex/0509008](#)].
- [78] N. Chen, T. Han, S. Su, W. Su, and Y. Wu, *Type-II 2HDM under the Precision Measurements at the Z-pole and a Higgs Factory*, *JHEP* **03** (2019) 023, [[arXiv:1808.02037](#)].
- [79] N. Chen, T. Han, S. Li, S. Su, W. Su, and Y. Wu, *Type-I 2HDM under the Higgs and Electroweak Precision Measurements*, *JHEP* **08** (2020) 131, [[arXiv:1912.01431](#)].
- [80] A. Sirlin and A. Ferroglia, *Radiative Corrections in Precision Electroweak Physics: a Historical Perspective*, *Rev. Mod. Phys.* **85** (2013), no. 1 263–297, [[arXiv:1210.5296](#)].
- [81] **ATLAS** Collaboration, *Combination of searches for non-resonant and resonant Higgs boson pair production in the $b\bar{b}\gamma\gamma$, $b\bar{b}\tau^+\tau^-$ and $b\bar{b}b\bar{b}$ decay channels using pp collisions at $\sqrt{s} = 13$ TeV with the ATLAS detector*, .
- [82] M. Misiak and M. Steinhauser, *Weak radiative decays of the B meson and bounds on M_{H^\pm} in the Two-Higgs-Doublet Model*, *Eur. Phys. J. C* **77** (2017), no. 3 201, [[arXiv:1702.04571](#)].
- [83] A. Arbey, F. Mahmoudi, O. Stal, and T. Stefaniak, *Status of the Charged Higgs Boson in Two Higgs Doublet Models*, *Eur. Phys. J. C* **78** (2018), no. 3 182, [[arXiv:1706.07414](#)].
- [84] T. Han, T. Li, S. Su, and L.-T. Wang, *Non-Decoupling MSSM Higgs Sector and Light Superpartners*, *JHEP* **11** (2013) 053, [[arXiv:1306.3229](#)].
- [85] P. Basler and M. Mühlleitner, *BSMPT (Beyond the Standard Model Phase Transitions): A tool for the electroweak phase transition in extended Higgs sectors*, *Comput. Phys. Commun.* **237** (2019) 62–85, [[arXiv:1803.02846](#)].